We are IntechOpen, the world's leading publisher of Open Access books Built by scientists, for scientists

6,900
Open access books available

185,000
International authors and editors

200M
Downloads

Our authors are among the

154
Countries delivered to

TOP 1%
most cited scientists

12.2%
Contributors from top 500 universities



WEB OF SCIENCE™

Selection of our books indexed in the Book Citation Index in Web of Science™ Core Collection (BKCI)

Interested in publishing with us?
Contact book.department@intechopen.com

Numbers displayed above are based on latest data collected.
For more information visit www.intechopen.com



Chapter 17

Carbon Nanotubes Influence on Spectral, Photoconductive, Photorefractive and Dynamic Properties of the Optical Materials

Natalia V. Kamanina

Additional information is available at the end of the chapter

http://dx.doi.org/10.5772/50843

1. Introduction

It is well known that optoelectronics, telecommunication systems, aerospace, and correction of amplitude-phase aberration schemes, as well as laser, display, solar energy, gas storage and biomedicine techniques are searching for the new optical materials and for the new methods to optimize their properties. So many scientific and research groups are involving in this process and are opening the wide aspects of different applications of new materials, especially optical ones. It has been going on last century that simple manufacturing, design, ecology points of view, etc. indicate good advantage of the nanostructured materials with improved photorefractive parameters among other organic and inorganic systems.

Really, it should be tell that photorefractive properties change is correlated with the spectral, photoconductive and dynamics ones. The change in nonlinear refraction and cubic nonlinearity reveals the modification of barrier free electron pathway and dipole polarizability. From one side it is connected with the change of the dipole moment and the charge carrier mobility, from other side, it is regarded to the change of absorption cross section. Thus, this feature shows the unique place of photorefractive characteristics among other ones in order to characterize the spectral, photoconductive, photorefractive and dynamic properties of the optical materials.

It should be mentioned that promising nanoobjects, such as the fullerenes, the carbon nanotubes (CNTs), the quantum dots (QDs), the shungites, and the graphenes permit to found different area of applications of these nanoobjects [1-6]. The main reason to use the fullerenes, shungites, and quantum dots is connected with their unique energy levels and high value of electron affinity energy. The basic features of carbon nanotubes and graphenes are

INTECH
open science | open minds

© 2013 Kamanina; licensee InTech. This is an open access article distributed under the terms of the Creative Commons Attribution License (http://creativecommons.org/licenses/by/3.0), which permits unrestricted use, distribution, and reproduction in any medium, provided the original work is properly cited.

regarded to their high conductivity, strong hardness of their C-C bonds as well as complicated and unique mechanisms of charge carrier moving.

These peculiarities of carbon nanoobjects and their possible optoelectronics, solar energy, gas storage, medicine, display and biology applications connecting with dramatic improvement of photorefractive, spectral, photoconductive and dynamic parameters will be under consideration in this paper. In comparison with other effective nanoobjects the mail accent will be given namely on carbon nanotubes (CNTs) and their unique features to modify the properties of the optical materials.

2. Experiment

The different experimental techniques have been used to study the properties of nanostructured materials.

To reveal the change of the photorefractive properties, as the systems under study the organic thin films based on conjugated monomer, polymer and liquid crystals sensitized with carbon nanotubes, fullerenes, shungites, graphenes oxides, or quantum dots have been chosen. Polyimides (PI), 2-cyclooctylamino-5-nitropyridine (COANP), *N*-(4-nitrophenyl)-(*L*)-prolinol (NPP), 2-(*N*-prolinol)-5-nitropyridine (PNP), nematic liquid crystals (NLCs) have been considered as organic matrixes. These conjugated systems are the good model with effective intramolecular charge transfer process which can be easy modify via sensitization by nanoobjects. Carbon nanotubes, fullerenes, shungites, graphenes oxides, quantum dots content was varied in the range of 0.003-5.0 wt.%. The solid thin films have been developed using centrifuge deposition. The general view of these films is shown in Fig.1. The thickness of the films was 2-5 micrometers. The LC cell thickness was 5-10 micrometers.

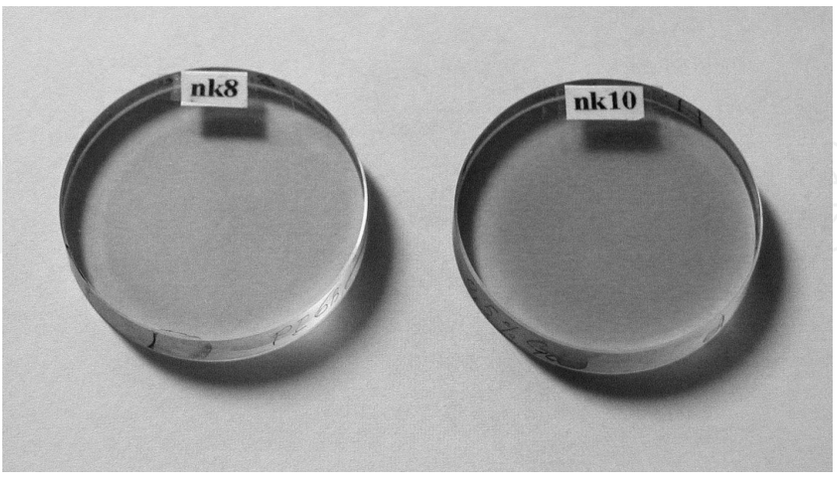


Figure 1. Photographs of samples of pure (nk8) and nanoobjects-containing (nk10) PI films.

The nanostructured LC films have been placed onto glass substrates covered with transparent conducting layers based on ITO contacts. The nanostructured monomer or polymer sol-

http://dx.doi.org/10.5772/50843

id films have been deposited on the substrate with ITO contact. For the electric measurements of volt-ampere parameters, gold contact has been put to the solid thin films upper side. The picture which can interpret the placement of the conducting contacts on the solid conjugated organic thin films is shown in Fig.2.

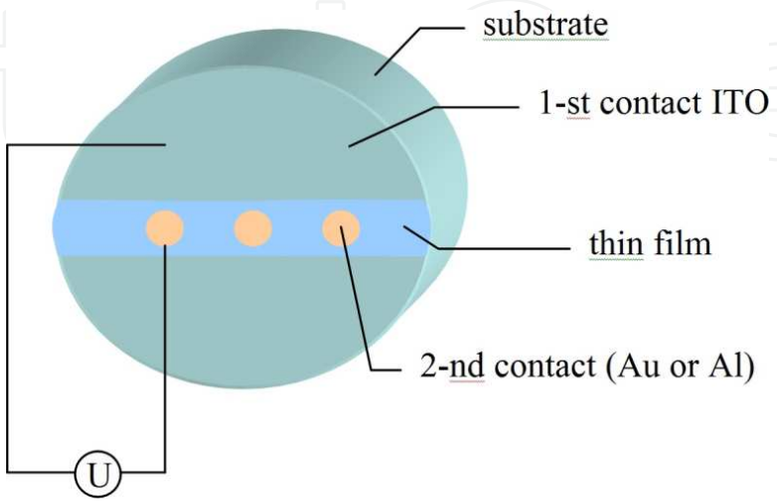


Figure 2. Interpretation of the solid thin films with the conducting layers

The bias voltage applied to the photosensitive polymer layers has been varied from 0 to 50 V. The current–voltage characteristics have been measured under the illumination conditions from dark to light. Voltmeter-electrometer B7—30 and Characteriscope—Z, type TR-4805 has been used for these photoconductive experiments.

The photorefractive characteristics have been studied using four-wave mixing technique analogous to paper [7]. The experimental scheme is shown in Fig.3.

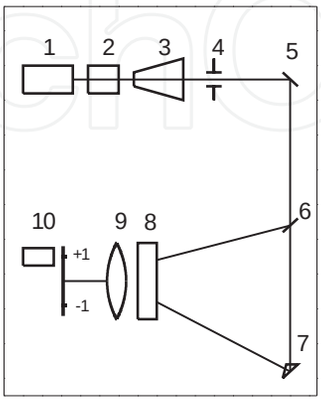


Figure 3. An experimental scheme: 1 – Nd-laser; 2 – second harmonic convertor; 3 – telescope; 4 – diaphragm; 5 – rotating mirror; 6 – beam-splitting mirror; 7 – prism; 8 – sample; 9 – lens; 10 - photodetector.

The second harmonic of pulsed Nd-laser at wave length of 532 nm has been used. The laser energy density has been chosen in the range of 0.005-0.9 J×cm^{-2}. The nanosecond laser regime with the pulse width of 10-20 ns has been applied. The amplitude-phase thin gratings have been recorded under Raman-Nath diffraction conditions according to which $\Lambda^{-1} \geq d$, where Λ^{-1} is the inverse spatial frequency of recording (i.e., the period of the recorded grating) and d is the film thickness. In the experiments the spatial frequency was in the range of 90-150 mm^{-1}.

The spectral characteristics have been tested using Perkin Elmer lambda 9 spectrophotometer. Dynamic features of nanoobjects-doped LC films have been studied via the four-wave mixing technique and the Frederick's scheme one. Atomic force microscopy (AFM) method using equipment of "NT-MDT" firm, "Bio47-Smena" in the "share-force" regime has been applied to analyze the diffraction relief into the solid conjugated nanostructured thin film.

3. Results and discussion

It should be noticed that previously, we demonstrated [5,6,8] the formation of barrier-free charge transfer pathways, increased dipole moment, and increased specific (per unit volume) local polarizability in some organic matrices doped with fullerenes, carbon nanotubes and quantum dots, where the formation of intermolecular complexes predominated over the intramolecular donor–acceptor interaction. The possible schemes of charge transfer between matrix organic molecule donor fragment and different efficient nanosensitizers including the additional graphene and shungites nanostructures are schematically shown in Fig. 4.

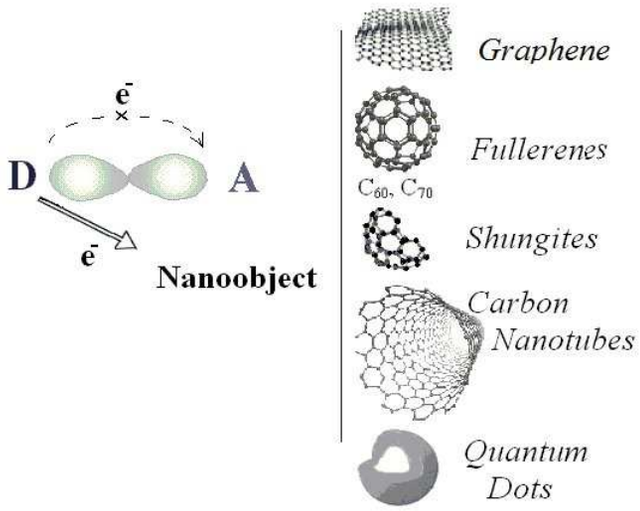


Figure 4. Schematic diagram of possible intermolecular charge transfer domination under intramolecular ones.

Analyzing the Fig.4, one can say that it is necessary to take into account that the charge transfer between matrix organic molecule donor fragment and nanasensitizers can be organ-

http://dx.doi.org/10.5772/50843

ized due to their high electron affinity energy (for example, electron affinity energy is close to 2 eV for shungites [9], to 2.65 eV for fullerenes [5,8] and to 3.8-4.2 eV for quantum dots [10]) that is more than the ones for intramolecular acceptor fragments (for example, electron affinity energy of COANP acceptor fragment is close to 0.54 eV [11] and to 1.14-1.4 eV for polyimide one [12]). Regarding graphenes it is necessary to take into account the high surface energy and planarity of the graphenes plane which can provoke to organize the charge transfer complex (CTC) with good advantage too. Regarding the CNTs it should be drawn the attention on the variety of charge transfer pathways, including those along and across a CNT, between CNTs, inside a multiwall CNT, between organic matrix molecules and CNTs, and between the donor and acceptor fragments of an organic matrix molecule.

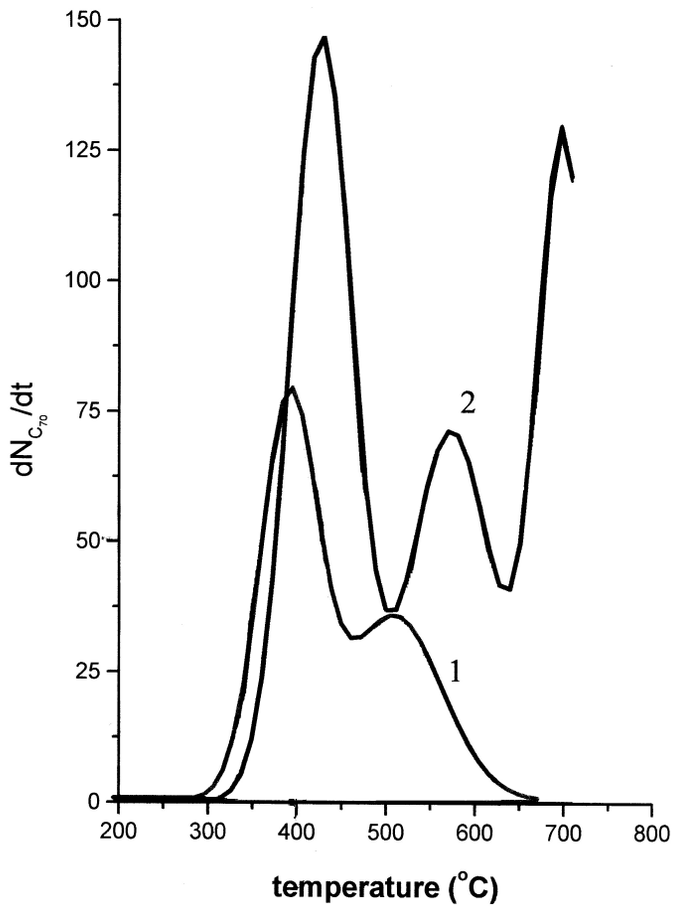


Figure 5. The rate of release of C_{70} molecules on heating of systems: (*1*) COANP with 5 wt % of C_{70} and (*2*) polyimide with 0.5 wt % of C_{70}

It should be noticed that some supporting CTC results for PIs and COANP systems sensitized with nanoobjects can be presented via mass-spectrometry experiments. It is easy to show the organization of CTC using fullerenes acceptor. Really, the mass spectroscopy data point to the effective CTC formation between fullerene and donor part of PI (triphenyla-

mine) and between fullerene and the HN group of COANP systems, respectively. For the 5 wt.% C_{70}-COANP film, mass spectrometry curve contains two peaks. The first one at 400 C corresponds to the release rate of fragments with free fullerene masses. The second one is shifted to the temperature range of 520 °C and associated with the decomposition temperature of the fullerene-HN group complex. For the 0.5 wt.% C_{70}-PI film, curve contains three peaks. The first one is observed also close to 400 C. The second peak is located at 560 °C and associated with the decomposition of fullerene- triphenylamine complex. It should be noticed that the melting temperature of these PIs is 700-1000 °C, thus, the third peak at the temperature higher 700 °C corresponds to the total decomposition of PI. Figure 5 presents the mass-spectrometry data.

By monitoring the diffraction response manifested in the laser scheme (see Fig.6); it is possible to study the dynamics of a photo-induced change in the refractive index of a sample and to calculate via [13] the nonlinear refraction and nonlinear third order optical susceptibility (cubic nonlinearity). An increase in the latter parameter characterizes a change in the specific (per unit volume) local polarizability and, hence, in the macroscopic polarization of the entire system.

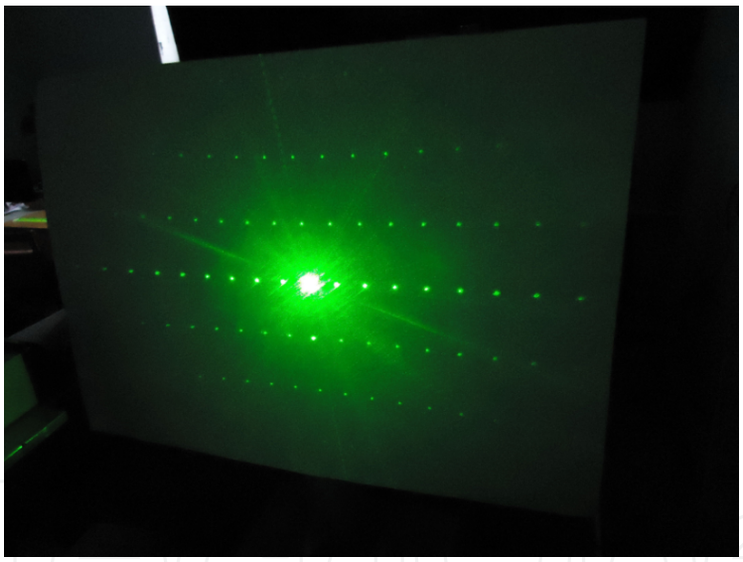


Figure 6. The visualization of the diffraction response in the organic films doped with nanoobjects.

The main results of this study are summarized in the Table 1 (Ref. 5,6,9,14-18) in comparison to the data of some previous investigations. An analysis of data presented in the Table 1 for various organic systems shows that the introduction of nanoobjects as active acceptors of electrons significantly influences the charge transfer under conditions where the intermolecular interaction predominates over the intramolecular donor–acceptor ones. Moreover, redistribution of the electron density during the recording of gratings in nanostructured materials changes the refractive index by at least one order of magnitude in comparision to that in the initial matrix. The diffusion of carriers from the bright to dark region during the laser recording of the interference pattern proceeds in three (rather than two) dimensions, which is

http://dx.doi.org/10.5772/50843

manifested by a difference in the distribution of diffraction orders along the horizontal and vertical axes (see Fig.6). Thus, the grating displacement takes place in a three dimensional (3D) medium formed as a result of the nanostructirization (rather than in a 2D medium).

Some atomic force microscopy data are supported the realization of 3D-media via development of complicated diffraction relief into the solid thin conjugated films after transfer from the reversible regime to the irreversible one. Figure 7 demonstrates this fact. Two types of diffraction replica, namely due to interference of laser beams onto the thin films surface and due to the diffraction of these beams inside the body of the nanostructured media have been presented.

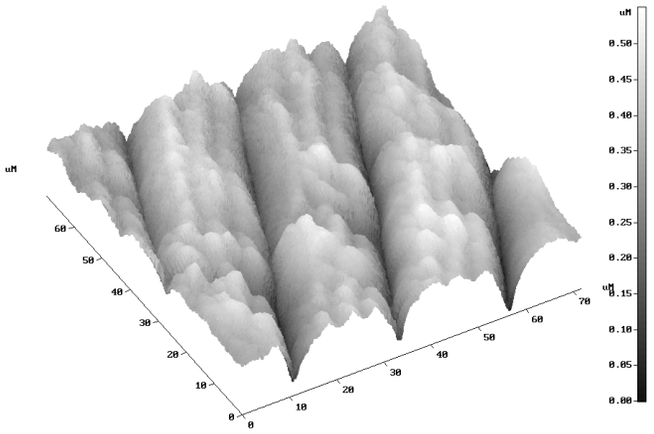


Figure 7. Demonstration of AFM evidence of new 3D-media development.

Using the obtained results, the nonlinear refraction n_2 and nonlinear third order optical susceptibility (cubic nonlinearity) $\chi^{(3)}$ for all systems have been calculated using a method described in [13,18]. In the current experiments using four-wave mixing technique, the nonlinear refraction coefficient and cubic nonlinearity (third order susceptibility) have been estimated via equations (1) and (2):

$$n_2 = \Delta n_i / I \tag{1}$$

$$\chi^{(3)} = n_2 n_0 c / 16\pi^2 \tag{2}$$

where I – is the irradiation intensity, n_o – is the linear refractive index of the media, c – is the speed of the light.

It was found that these parameters fall within $n_2 = 10^{-10}$–10^{-9} cm^2/W and $\chi^{(3)} = 10^{-10}$–10^{-9} cm^3/erg.

Moreover, it should be remained, that optical susceptibility $\chi^{(n)}$, from fundamental point of view, directly connected with the dipole system polarizability $^{(n)}$ via equation (3) written in the paper [19]:

$$\chi^{(n)} = \alpha^{(n)} / \upsilon \tag{3}$$

where $\alpha^{(n)}$ – dipole polarizability and υ – local volume.

Therefore, using the fact that polarizability of all structures can be accumulated from local volumes, it can be found that increased micropolarization of system (see eq.4) will predict the dynamic properties improvement and high electro-optical response speed.

$$P = \chi^{(1)} E + \chi^{(2)} E^2 + \chi^{(3)} E^3 + \ldots + \chi^{(n)} E^n + \ldots \tag{4}$$

It should be mentioned (see Table 1) that the larger nonlinear optical parameters have been found for CNTs-doped organic systems or CNTs-nanofibers-doped ones. It is natural to suggest (see Fig.8) that variations of the length, of the surface energy, of the angle of nanoobject orientation relative to the intramolecular donor can significantly change the pathway of charge carrier transfer, which will lead to changes in the electric field gradient, dipole moment (proportional to the product of charge and distance), and mobility of charge carriers.

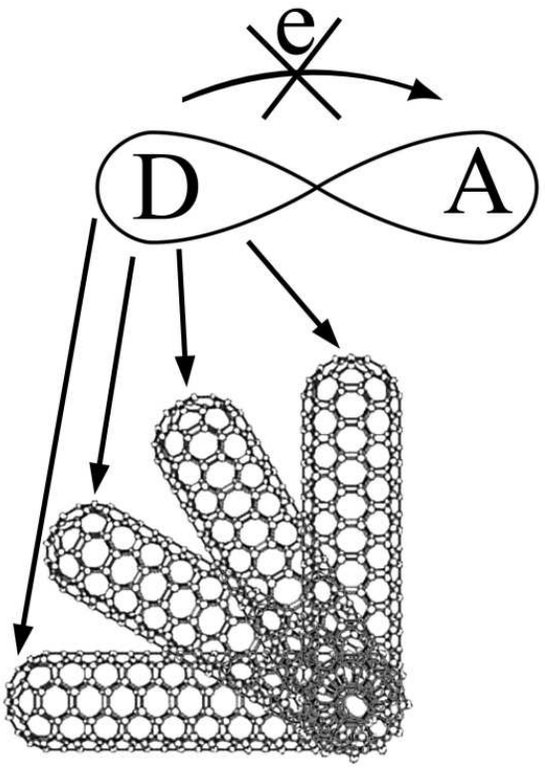


Figure 8. Schematic diagram of possible charge transfer pathways depending on the arrangement of introduced intermolecular acceptor relative to the intramolecular donor

http://dx.doi.org/10.5772/50843

In addition, the barrier free charge transfer will be influenced by competition between the diffusion and drift of carriers during the creation of diffraction patterns with various periods and, hence, differing charge localization at the grating nodes and antinodes. Indeed, in the case of a nanocomposite irradiated at small spatial frequencies (large periods of recorded grating), a drift mechanism of the carrier spreading in the electric field of an intense radiation field will moist probably predominate, while at large spatial frequencies (short periods of recorded grating) the dominating process is diffusion. This also naturally accounts for the aforementioned discrepancy of published data on photoinduced changes in the refractive index of nanocomposites, greater values of which were observed (see, e.g., data presented in the table for systems doped with CNTs and MIG nanofibers) at smaller spatial frequencies. Lower values of photoinduced changes in the refractive index of nanocomposites were observed at high spatial frequencies. This evidence predicts the strong correlations between photorefractive and photoconductive parameters.

To support the evidence on correlation between photorefractive and photoconductive features of the materials studied, the volt-current characteristics for nanoobjects-doped solid thin films and pure ones has been measured. After that charge carrier mobility has been estimated using the Child–Langmuir current–voltage relationship [20] following the formula (5) shown below:

$$\mu = 10^{13} I d^{3} \times \varepsilon^{-1} V^{-1} \tag{5}$$

For example, one can calculate the absolute values of the charge carrier mobility in pure and fullerene-modified PI samples. The results of these calculations show that the introduction of fullerenes leads to a tenfold increase in the mobility. The absolute values were estimated for a bias voltage of 10 V, a film thickness of d = 2 μm, a dielectric constant of ε ~ 3.3, a fullerene content of about 0.2 wt % C_{70}, and an upper electrode contact area with a diameter of 2 mm. Under these conditions, the carrier mobility in a fullerene-modified polyimide PI film is ~0.3 × 10^{-4} cm^2/(V s), while the analogous value for pure PI is ~0.17 × 10^{-5} cm^2/(V s). These values well agree with the data reported in [21], where it was demonstrated that the carrier mobility in pure PI films ranges in the interval from 10^{-7} to 0.5 × 10^{-5} cm^2/(V s). Relationship (5) used for the estimation of charge carrier mobility is valid in the case of currents limited by the space charge. This situation is characteristic of most of the conjugated organic structures (in particular, PIs) in which the charge transfer processes are additionally determined by traps, although formula (5) contains no terms dependent on the illumination intensity. However, taking into account the aforementioned equality of the activation energies of conductivity and mobility in PIs, the results of calculations of the relative changes in the carrier mobility probably adequately reflect the general trends in mobility variations. This behavior does not contradict the pattern of changes in the mobility observed for the other conjugated organic systems, for example, for the fullerene–carbazole one [22].

We have also calculated the relative values of the charge carrier mobility μ and estimated that two orders of magnitude differences of charge carrier mobility for the pure and nanoob-

jects-doped films has been found. Moreover, the following relation for the charge carrier mobility has been proposed:

$$\mu_{\text{pure organic systems}} < \cdot \mu_{C70,C60} < \cdot \mu_{CNT,QD} \quad (6)$$

The observation of the increase of charge carrier mobility, high refractive index and high value of cubic nonlinearities predicts that the nonlinear optical and the dynamic feature of the nanostructured conjugated materials can be optimized via nanostructurization with good advantage. It should be noted that classical inorganic nonlinear volume media (including BSO, $LiNbO_3$, etc.) exhibit significantly lower nonlinearity, while bulk silicon based materials have nonlinear characteristics analogous to those of the organic thin film nanoobjects-doped materials under consideration.

Structure	Content of dopants, wt.%	Wavelength, nm	Energy density, Jcm^{-2}	Spatial frequency, mm^{-1}	Laser pulse duration, ns	Laser-induced change in the refractive index, (n	References
NPP	0	532	0.3	100	20	$0.65x10^{-3}$	[14]
NPP+C_{60}	1	532	0.3	100	20	$1.65x10^{-3}$	[14]
NPP+C_{70}	1	532	0.3	100	20	$1.2x10^{-3}$	[14]
PNP*	0	532	0.3	100	20	*	
PNP+C_{60}	1	532	0.3	100	20	$0.8x10^{-3}$	[14]
PI	0	532	0.6	90-100	10-20	10^{-4}-10^{-5}	[5]
PI+malachite green dye	0.2	532	0.5-0.6	90-100	10-20	$2.87x10^{-4}$	[5]
PI+graphene oxides	0.1	532	0.2	100	10	$3.4x10^{-3}$	present
PI+graphene oxides	0.2	532	0.28-0.3	100	10	$3.65x10^{-3}$	present
PI+shungites	0.1	532	0.6	150	10	$3.1x10^{-3}$	present
PI+shungites	0.2	532	0.063-0.1	150	10	$5.3x10^{-3}$	[9,15]
PI+C_{60}	0.2	532	0.5-0.6	90-100	10-20	$4.2x10^{-3}$	[5]
PI+C_{70}	0.2	532	0.6	90-100	10-20	$4.68x10^{-3}$	[5]
PI+C_{70}	0.5	532	0.6	90-100	10-20	$4.87x10^{-3}$	[5]
PI+C_{70}	0.1-0.5	1315	0.2–0.8	100	50	$\sim10^{-3}$	[14]

http://dx.doi.org/10.5772/50843

PI+quantum dots based on CdSe(ZnS)	0.003	532	0.2-0.3	100	10	$2.0x10^{-3}$	[10]
PI+CNTs	0.1	532	0.5-0.8	90-100	10-20	$5.7x10^{-3}$	[6]
PI+ CNTs	0.05	532	0.3	150	20	$4.5x10^{-3}$	[6,14]
PI+ CNTs	0.07	532	0.3	150	20	$5.0x10^{-3}$	[6,14]
PI+ CNTs	0.1	532	0.3	150	20	$5.5x10^{-3}$	[6,14]
PI + double-walled carbon nanotube powder	0.1	532	0.1	100	10	$9.4x10^{-3}$	[15]
PI + double-walled carbon nanotube powder	0.1	532	0.1	150	10	$7.0x10^{-3}$	[15]
PI+ mixture of CNT and nanofibers (type MIG)	0.1	532	0.3-0.6	90-100	10	$11.7x10^{-3}$	[15]
PI+ mixture of CNT and nanofibers (type MIG)	0.1	532	0.3-0.6	150	10	$11.2x10^{-3}$	[15]
Polymer-dispersed LC based on PI–C_{70} complex	0.2	532	0.1	90-100	10	$1.2x\ 10^{-3}$	[10]
COANP	0	532	0.9	90-100	10-20	10^{-5}	[14]
COANP+ TCNQ**	0.1	676	2.2 Wcm^{-2}			$2x10^{-5}$	[16]
COANP+C_{60}	5	532	0.9	90-100	10-20	$6.21x10^{-3}$	[14]
COANP+C_{70}	0.5	532	0.6	100	10	$5.1x10^{-3}$	present
COANP+C_{70}	5	532	0.9	90-100	10-20	$6.89x10^{-3}$	[14]
Polymer-dispersed LC	0.5	532	30×10^{-3}	100	10	1.2×10^{-3}	present

based on COANP–C_{70} complex							
Polymer-dispersed LC based on COANP–C_{70} complex	5	532	17.5×10^{-3}	100	20	1.4×10^{-3}	[17]
Polymer-dispersed LC based on COANP–nanotubes	0.1	532	30×10^{-3}	100	10	2.8×10^{-3}	present
Polymer-dispersed LC based on COANP–nanotubes	0.5	532	18.0×10^{-3}	90-100	10-20	3.2×10^{-3}	[18]

Table 1. Laser-induced change in the refractive index in some organic structures doped with nanoobjects. * The diffraction efficiency has not detected for these systems at this energy density. ** Dye TCNQ - 7,7,8,8,-tetracyanoquinodimethane – has been used in the paper [16].

4. Conclusion

Thus, analysis of the obtained results leads to the following conclusions:

- Doping with nanoobjects significantly influences the photorefractive properties of nanobjects-doped organic matrices. An increase in the electron affinity (cf. shungite, fullerenes, QDs) and specific area (cf. QDs, CNTs, nanofilers) implies a dominant role of the intermolecular processes leading to an increase in the dipole moment, local polarizability (per unit volume) of medium, and mobility of charge carriers.
- A change in the distance between an intramolecular donor and intermolecular acceptor as a result of variation of the arrangement (rotation) of the introduced nanosensitizer leads to changes on the charge transfer pathway in the nanocomposite.
- The variations of the length, of the surface energy, of the angle of nanoobject orientation relative to the intramolecular donor fragment of matrix organics can significantly change the pathway of charge carrier transfer, which will lead to changes in the electric field gradient and dipole moment.
- Different values of nonlinear optical characteristics in systems with the same sensitizer type and concentration can be related to a competition between carrier drift and diffusion processes in a nanocomposite under the action of laser radiation.

http://dx.doi.org/10.5772/50843

- Special role of the dipole moment as a macroscopic parameter of a medium accounts for a relationship between the photorefraction and the photoconductivity characteristics.
- The photorefractive parameters change can be considered as the indicator of following dynamic and photoconductive characteristics change.

As the result of this discussion and investigation, new area of applications of the nanostructured materials can be found in the optoelectronics and laser optics, medicine, biology, telecommunications, display, microscopy technique, etc. Moreover, the nanostructured materials can be used for example, for development of 3D media with high density of recording information, as sensor in the gas storage and impurity testing, as photosensitive layer in the spatial light modulators, convertors, limiters, etc. devices.

Acknowledgements

The author would like to thank their Russian colleagues: Prof. N. M. Shmidt (Ioffe Physical-Technical Institute, St.-Petersburg, Russia), Prof. E.F.Sheka (University of Peoples' Friendship, Moscow, Russia), Dr.N.N.Rozhkova (Institute of Geology, Karelian Research Centre, RAS), Dr.A.I.Plekhanov (Institute of Automation and Electrometry SB RAS, Novosibirsk, Russia), Dr.V.I.Studeonov and Dr.P.Ya.Vasilyev (Vavilov State Optical Institute, St.-Petersburg, Russia), as well as foreign colleagues: Prof. Francois Kajzar (Université d'Angers, Angers, France), Prof. D.P. Uskokovic (Institute of Technical Sciences of the Serbian Academy of Sciences and Arts, Belgrade, Serbia), Prof. I.Kityk (Politechnica Czestochowska, Czestochowa, Poland), Dr. R.Ferritto (Nanoinnova Technologies SL, Madrid, Spain) for their help in discussion and study at different their steps. The presented results are correlated with the work supported by Russian Foundation for Basic Researches (grant 10-03-00916, 2010-2012).

Author details

Natalia V. Kamanina[1*]

Address all correspondence to: nvkamanina@mail.ru

1 Vavilov State Optical Institute, 12, Birzhevaya Line, St. Petersburg, , Russia

References

[1] Couris, S., Koudoumas, E., Ruth, A. A., & Leach, S. (1995). Concentration and wavelength dependence of the effective third-order susceptibility and optical limiting of C_{60} in toluene solution. *J. Phys. B: At. Mol. Opt. Phys.*, 8, 4537-4554.

[2] Robertson, J. (2004). Realistic applications of CNTs. .*Mater. Today*, 7, 46-52.

[3] Lee, Wei, & Chen, Hsu-Chih. (2003). Diffraction efficiency of a holographic grating in a liquid-crystal cell composed of asymmetrically patterned electrodes. *Nanotechnology*, 14, 987-990.

[4] Buchnev, Oleksandr, Dyadyusha, Andriy, Kaczmarek, Malgosia, Reshetnyak, Victor, & Reznikov, Yuriy. (2007). Enhanced two-beam coupling in colloids of ferroelectric nanoparticles in liquid crystals. J. Opt. Soc. Am. B/ , 24(7), 1512-1516.

[5] Kamanina, N. V., Emandi, A., Kajzar, F., & Attias, Andre´-Jean. (2008). Laser-Induced Change in the Refractive Index in the Systems Based on Nanostructured Polyimide: Comparative Study with Other Photosensitive Structures. *Mol. Cryst. Liq. Cryst.*, 486, 1-11.

[6] Kamanina, N. V., Serov, S. V., Savinov, V. P., & Uskoković, D. P. (2010). Photorefractive and photoconductive features of the nanostructured materials. *International Journal of Modern Physics B (IJMPB)*, 24(6-7), 695-702.

[7] Kamanina, N. V., & Vasilenko, N. A. (1997). Influence of operating conditions and of interface properties on dynamic characteristics of liquid-crystal spatial light modulators. *Opt. Quantum Electron.*, 29, 1-9.

[8] Kamanina, N. V. (2005). Fullerene-dispersed liquid crystal structure: dynamic characteristics and self-organization processes. *Physics-Uspekhi*, 48, 419-427.

[9] Kamanina, N. V., Serov, S. V., Shurpo, N. A., & Rozhkova, N. N. (2011). Photoinduced Changes in Refractive Index of Nanostructured Shungite-Containing Polyimide Systems. *Technical Physics Letters*, 37(10), 10(10), 949-951.

[10] Kamanina, N. V., Shurpo, N. A., Likhomanova, S. V., Serov, S. V., Ya, P., Vasilyev, V. G., Pogareva, V. I., Studenov, D. P., & Uskokovic, . (2011). Influence of the Nanostructures on the Surface and Bulk Physical Properties of Materials. *ACTA PHYSICA POLONICA A*, 119(2), 2(2), 256-259.

[11] Kamanina, N. V., & Plekhanov, A. I. (2002). Mechanisms of optical limiting in fullerene-doped conjugated organic structures demonstrated with polyimide and COANP molecules. *Optics and Spectroscopy*, 93(3), 408-415.

[12] Cherkasov, Y. A., Kamanina, N. V., Alexandrova, E. L., Berendyaev, V. I., Vasilenko, N. A., & Kotov, B. V. (1998). Polyimides: New properties of xerographic, thermoplastic, and liquid-crystal structures. (SPIE International Symposium on Optical Science, Engineering and Instrumentation, San Diego, CA, USA, 1998) Proceed. of SPIE , 3471, 254-260.

[13] Akhmanov, S. A., & Nikitin, S. F. (1998). Physical Optics. (Izdat. Mos. Gos. Univ., Moscow, 1998) [in Russian].

http://dx.doi.org/10.5772/50843

[14] Kamanina, N. V., Vasilyev Ya, P., Serov, S. V., Savinov, V. P., Bogdanov. Yu, K., & Uskokovic, D. P. (2010). Nanostructured Materials for Optoelectronic Applications. *Acta Physica Polonica A*, 117(5), 786-790.

[15] Kamanina, N. V., Serov, S. V., Shurpo, N. A., Likhomanova, S. V., Timonin, D. N., Kuzhakov, P. V., Rozhkova, N. N., Kityk, I. V., Plucinski, K. J., & Uskokovic, D. P. (2012). Polyimide-fullerene nanostructured materials for nonlinear optics and solar energy applications. J Mater Sci: Mater Electron DOI: 10.1007/s10854-012-0625-9, published on-line 26 January 2012.

[16] Ch Bosshard. Bosshard., K., Sutter, P., & Chapuis. Günter, G. (1989). Linear- and nonlinear-optical properties of 2 -cyclooctylamino-5-nitropyridine. *J. Opt. Soc. Am.*, B6, 721-725.

[17] Kamanina, N. V. (2002). Optical investigations of a C_{70}-doped 2-cyclooctylamino-5-nitropyridine-liquid crystal system. *Journal of Optics A: Pure and Applied Optics*,, 4(4), 4(4), 571-574.

[18] Kamanina, N. V., & Uskokovic, D. P. (2008). Refractive Index of Organic Systems Doped with Nano-Objects. *Materials and Manufacturing Processes*, 23, 552-556.

[19] Chemla, D. S., & Zyss, J. (1987). Nonlinear Optical Properties of Organic Molecules and Crystals . (Orlando Academic Press, 1987), Translated into Russian, Moscow: Mir, 1989., 2

[20] Gutman, F., & Lyons, L. E. (1967). Organic Semiconductors. Wiley, New York.

[21] Mylnikov, V. S. (1994). in Advances in Polymer Science. Photoconducting Polymers/ Metal-Containing Polymers Springer-Verlag Berlin , 115, 3-88.

[22] Wang, Y., & Suna, A. (1997). Fullerenes in Photoconductive Polymers. Charge Generation and Charge Transport. *J. Phys. Chem.*, B 101, 5627-5638.

IntechOpen

IntechOpen